Three-body scattering hypervolume of identical fermions in one dimension

Zipeng Wang and Shina Tan*
International Center for Quantum Materials, Peking University, Beijing 100871, China

(Received 27 February 2023; revised 11 July 2023; accepted 13 July 2023; published 6 September 2023)

We study the zero-energy collision of three identical spin-polarized fermions with short-range interactions in one dimension. We derive the asymptotic expansions of the three-body wave function when the three fermions are far apart or one pair and the third fermion are far apart, and the three-body scattering hypervolume D_F appears in the coefficients of such expansions. If the two-body interaction is attractive and supports two-body bound states, D_F acquires a negative imaginary part related to the amplitudes of the outgoing waves describing the departure of the resultant bound pair and the remaining free fermion. For weak interaction potentials, we derive an approximate formula of the hypervolume by using the Born expansion. For the square-barrier and the square-well potentials and the Gaussian potential, we solve the three-body Schrödinger equation to compute D_F numerically. We also calculate the shifts of energy and of pressure of spin-polarized one-dimensional Fermi gases due to a nonzero D_F and the three-body recombination rate in one dimension.

DOI: 10.1103/PhysRevA.108.033306

I. INTRODUCTION

One-dimensional (1D) quantum gases can be experimentally realized by applying strong confinement in two transverse directions and allow free motion along the longitudinal direction [1–10]. 1D quantum gases are very different from the ordinary three-dimensional (3D) quantum gases [11,12].

The three-body problem in 1D has been studied for many years [13–20]. In this paper, we define and study the *three-body scattering hypervolume* of identical spin-polarized fermions in 1D. The scattering hypervolume is a three-body analog of the two-body scattering length [21], which can be extracted from the wave function of two particles colliding at zero energy. If the interaction is short ranged, i.e., the interaction potential vanishes beyond a finite pairwise distance r_e, the wave function of two particles colliding at zero energy in 1D is

$$\phi_l(s) = (|s| - a_l)Y_l(s) \tag{1}$$

at $|s| > r_e$ in the center-of-mass frame, where a_l is the two-body scattering length in 1D, s is the difference of the coordinates of the two particles, and l can be 0 or 1 for s-wave collisions or p-wave collisions, respectively. $Y_0(s) = 1$ and $Y_1(s) = \mathrm{sgn}(s)$. Here $\mathrm{sgn}(s)$ is the sign function. $\mathrm{sgn}(s) = 1$ for $s > 0$, $\mathrm{sgn}(s) = 0$ for $s = 0$, and $\mathrm{sgn}(s) = -1$ for $s < 0$.

For particles in higher-dimensional spaces, people have defined and studied the three-body scattering hypervolume in various systems [21–29]. The three-body scattering hypervolumes have been defined and studied for identical bosons in 3D [21–24,27], distinguishable particles in 3D [25,26], identical spin-polarized fermions in 3D [28] or in two dimensions (2D) [29]. In this paper, we define the scattering hypervolume D_F of identical spin-polarized fermions in 1D by studying the wave function of three such fermions colliding at zero energy, and study its analytical and numerical calculations and its physical implications. Our results may be applicable to ultracold atomic Fermi gases confined in one dimension.

This paper is organized as follows. In Sec. II we define the two-body p-wave special functions. In Sec. III we derive the asymptotic expansions of the three-body wave function for zero energy collision. The scattering hypervolume D_F appears in the coefficients in these expansions. In Sec. IV, we derive an approximate formula of D_F for weak interaction potentials by using the Born expansion. For the square-barrier and the square-well potentials and the Gaussian potential we numerically compute D_F for various interaction strengths. In Sec. V we consider the dilute spin-polarized Fermi gas in 1D and derive the shifts of its energy and pressure due to a nonzero D_F. In Sec. VI, we derive the formula for the three-body recombination rate of the dilute spin-polarized Fermi gas in 1D in terms of the imaginary part of D_F.

II. TWO-BODY SPECIAL FUNCTIONS

For identical spin-polarized fermions in 1D, the s-wave two-body scattering is forbidden due to Fermi statistics, and only the p-wave scattering is permitted. The two-fermion scattering wave function Φ in the center-of-mass frame with collision energy $E = \hbar^2k^2/m$, where m is the mass of each fermion and $\hbar$ is Planck's constant over 2π, satisfies the following Schrödinger equation:

$$\frac{d^2\Phi(s)}{ds^2} + \left[k^2 - \frac{mV(s)}{\hbar^2}\right]\Phi(s) = 0, \tag{2}$$

where $V(s)$ is the two-body interaction potential. We assume that $V(s)$ is an even function of s, namely $V(s) = V(|s|)$, and that it vanishes at $|s| > r_e$. At $|s| > r_e$, Eq. (2) is simplified as

*shinatan@pku.edu.cn

$d^2\Phi/ds^2 + k^2\Phi = 0$, and its solution is

$$\Phi(s) = A\sin(k|s| + \delta_p)\mathrm{sgn}(s), \tag{3}$$

where δ_p is the p-wave scattering phase shift which obeys the effective range expansion in 1D [30,31]:

$$k\cot\delta_p = -\frac{1}{a_p} + \frac{1}{2}r_p k^2 + \frac{1}{4!}r_p' k^4 + O(k^6). \tag{4}$$

Here a_p is the p-wave scattering length in 1D, r_p is the p-wave effective range, and r_p' is the p-wave shape parameter.

If the collision energy is small, namely $|k| \ll 1/r_e$, the wave function can be expanded in powers of k^2:

$$\Phi^{(k)}(s) = \phi(s) + k^2 f(s) + k^4 g(s) + O(k^6), \tag{5}$$

where $\phi, f, g, \dots$ are called the two-body special functions and they satisfy the equations [25,28]

$$\widetilde{H}\phi = 0, \quad \widetilde{H}f = \phi, \quad \widetilde{H}g = f, \dots, \tag{6}$$

where $\widetilde{H}$ is defined as

$$\widetilde{H} \equiv -\frac{d^2}{ds^2} + \frac{m}{\hbar^2}V(s). \tag{7}$$

The two-body special functions at $|s| > r_e$ can be extracted from Eq. (3). By choosing the coefficient $A = -a_p/\sin\delta_p$, we get

$$\phi(s) = (|s| - a_p)\mathrm{sgn}(s), \tag{8a}$$

$$f(s) = \left(-\frac{|s|^3}{6} + \frac{a_p}{2}|s|^2 - \frac{1}{2}a_p r_p|s|\right)\mathrm{sgn}(s), \tag{8b}$$

$$g(s) = \left(\frac{|s|^5}{120} - \frac{a_p}{24}|s|^4 + \frac{a_p r_p}{12}|s|^3 - \frac{a_p r_p'}{24}|s|\right)\mathrm{sgn}(s) \tag{8c}$$

for $|s| > r_e$.

III. ASYMPTOTICS OF THE THREE-BODY WAVE FUNCTION

We consider the collision of three fermions with finite range interactions at zero energy in the center-of-mass frame. The three-body wave function $\Psi(x_1, x_2, x_3)$ satisfies the following Schrödinger equation:

$$-\sum_{i=1}^{3}\frac{\hbar^2}{2m}\frac{\partial^2\Psi}{\partial x_i^2} + \sum_{i=1}^{3}V(s_i)\Psi + U(s_1, s_2, s_3)\Psi = 0, \tag{9}$$

where x_i is the coordinate of the ith fermion, and $s_i \equiv x_j - x_k$. The indices $(i, j, k) = (1, 2, 3)$, (2,3,1), or (3,1,2). U is the three-body potential. We assume that the interactions among these fermions depend only on the interparticle distances. The total momentum of the three fermions is zero such that the wave function is translationally invariant. We assume that $V(s_i) = 0$ if $|s_i| > r_e$, and that $U(s_1, s_2, s_3) = 0$ if $|s_1|$, $|s_2|$, or $|s_3|$ is greater than r_e.

To uniquely determine the wave function for the zero energy collision, we need to also specify the asymptotic behavior of Ψ when the three particles are far apart. Suppose that the leading-order term Ψ_0 in the wave function scales as B^p at large B, where $B = [(s_1^2 + s_2^2 + s_3^2)/2]^{1/2}$ is the hyperradius. Ψ_0 should also satisfy the free Schrödinger equation $(\partial_1^2 + \partial_2^2 + \partial_3^2)\Psi_0 = 0$. The most important channel for zero-energy collisions, for purposes of understanding ultracold collisions, should be the one with the minimum value of p [28]. We find that the minimum value of p for three identical fermions in 1D is $p_{\min} = 3$, and the leading-order term Ψ_0 is

$$\Psi_0 = s_1 s_2 s_3 = (x_2 - x_3)(x_3 - x_1)(x_1 - x_2). \tag{10}$$

One can check that Ψ_0 in Eq. (10) is translationally invariant and it obeys the Fermi statistics.

Like what we did in previous works [21,25,28,29], we derive the corresponding 111 expansion and 21 expansion for the three-body wave function Ψ. When the three particles are all far apart from each other, such that the pairwise distances $|s_1|$, $|s_2|$, $|s_3|$ go to infinity simultaneously for any fixed ratio $s_1 : s_2 : s_3$, we expand Ψ in powers of $1/B$ and this expansion is called the 111 expansion. When one fermion is far away from the other two, but the two fermions are held at a fixed distance s_i, we expand Ψ in powers of $1/R_i$, where $R_i = x_i - (x_j + x_k)/2$ is a Jacobi coordinate, and this is called the 21 expansion. These expansions can be written as

$$\Psi = \sum_{p=-3}^{\infty}\mathcal{T}^{(-p)}(x_1, x_2, x_3), \tag{11a}$$

$$\Psi = \sum_{q=-2}^{\infty}\mathcal{S}^{(-q)}(R, s), \tag{11b}$$

where $\mathcal{T}^{(-p)}$ scales like B^{-p}, $\mathcal{S}^{(-q)}$ scales like R^{-q}, and $R \equiv R_i$ and $s \equiv s_i$ for any i. $\mathcal{T}^{(-p)}$ satisfies the free Schrödinger equation outside of the interaction range:

$$-\left(\frac{\partial^2}{\partial s^2} + \frac{3}{4}\frac{\partial^2}{\partial R^2}\right)\mathcal{T}^{(-p)} = 0. \tag{12}$$

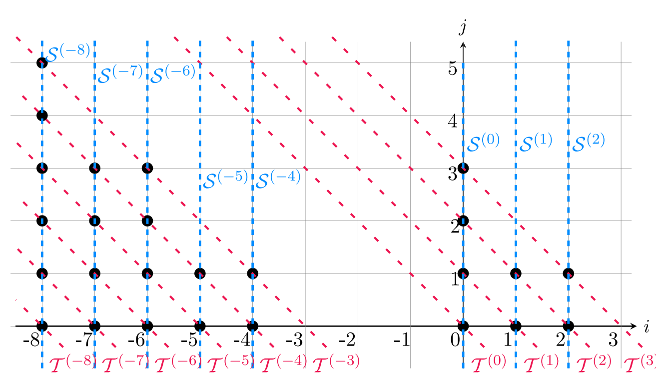

FIG. 1. Diagram of the points representing $t^{(i,j)}$ on the (i, j) plane. Each point with coordinates (i, j) represents $t^{(i,j)}$ which scales like $R^i s^j$. Thick dots represent those points at which $t^{(i,j)} \neq 0$. The term $\mathcal{T}^{(-p)}$ in the 111 expansion is represented by a red dashed line satisfying the equation $i + j = -p$. The term $\mathcal{S}^{(-q)}$ in the 21 expansion is represented by a blue dashed line satisfying the equation $i = -q$.

If one fermion is far away from the other two, Eq. (9) becomes

$$\left(\widetilde{H}-\frac{3}{4}\frac{\partial^2}{\partial R^2}\right)\Psi=0, \tag{13}$$

where $\widetilde{H}$ is defined in Eq. (7), but the d/ds should be replaced by $\partial/\partial s$ here. Therefore, $\mathcal{S}^{(-q)}$ satisfies the following equations:

$$\widetilde{H}\mathcal{S}^{(2)}=0,\quad \widetilde{H}\mathcal{S}^{(1)}=0,$$
$$\widetilde{H}\mathcal{S}^{(-q)}=\frac{3}{4}\frac{\partial^2}{\partial R^2}\mathcal{S}^{(-q+2)}\ (q\geqslant 0). \tag{14}$$

To derive the two expansions, we start from the leading-order term in the 111 expansion (which fixes the overall amplitude of Ψ):

$$\mathcal{T}^{(3)}=\Psi_0=\tfrac{1}{4}s^3-sR^2. \tag{15}$$

We then first derive $\mathcal{S}^{(2)}$, and then derive $\mathcal{T}^{(2)}$, and then derive $\mathcal{S}^{(1)}$, and then derive $\mathcal{T}^{(1)}$, and so on, all the way until $\mathcal{S}^{(-8)}$. At every step, we require the 111 expansion and the 21 expansion to be consistent in the region $r_e\ll|s|\ll|R|$, in which the wave function has a double expansion:

$$\Psi=\sum_{i,j}t^{(i,j)}, \tag{16}$$

where $t^{(i,j)}$ scales as $R^i s^j$, and

$$\mathcal{T}^{(-p)}=\sum_{i}t^{(i,-p-i)}, \tag{17}$$

$$\mathcal{S}^{(-q)}=\sum_{j}t^{(-q,j)}. \tag{18}$$

In Fig. 1 we show the points on the $(i,\,j)$ plane for which $t^{(i,j)}$ is nonzero. Our resultant 111 expansion is

$$\begin{aligned}\Psi={}&s_1s_2s_3\left(1-\frac{3\sqrt{3}D_F}{2\pi B^6}\right)+\sum_{i=1}^{3}\Bigg[-a_pB^2\cos(2\Theta_i)\mathrm{sgn}(s_i)-\frac{6}{\pi}a_p^2B\theta_i\sin\theta_i\mathrm{sgn}(s_i)+\frac{3}{4}\left(2a_p^3+a_p^2r_p\right)\mathrm{sgn}(s_i)\\&-\frac{3\sqrt{3}a_pD_F}{2\pi B^4}\cos(4\Theta_i)\mathrm{sgn}(s_i)-\frac{18\sqrt{3}a_p^2D_F}{\pi^2B^5}\theta_i\sin(5\theta_i)\mathrm{sgn}(s_i)\\&+\frac{45\sqrt{3}D_F}{4\pi B^6}\left(2a_p^3+a_p^2r_p\right)\cos(6\Theta_i)\mathrm{sgn}(s_i)\\&+\frac{405\sqrt{3}}{2\pi^2B^7}a_p^3r_pD_F\theta_i\sin(7\theta_i)\mathrm{sgn}(s_i)-\frac{945\sqrt{3}D_F}{32\pi B^8}\left(6a_p^3r_p^2+a_p^2r_p'\right)\cos(8\Theta_i)\mathrm{sgn}(s_i)\Bigg]+O(B^{-9}),\end{aligned} \tag{19}$$

where D_F is the three-body scattering hypervolume. The coefficient in $\mathcal{T}^{(-3)}$ is chosen such that $(\partial_s^2+\frac{3}{4}\partial_R^2)\mathcal{T}^{(-3)}=\frac{3}{4}D_F[\delta'(s)\delta''(R)-\frac{4}{9}\delta'''(s)\delta(R)]$, and this coefficient will simplify the expression for the shift of the energy of three fermions along a periodic line; see Eq. (61). Θ_i is called the hyperangle and is defined via the following equations:

$$\frac{\sqrt{3}}{2}s_i=B\cos\Theta_i,\quad R_i=B\sin\Theta_i. \tag{20}$$

One can verify that the three hyperangles satisfy $\Theta_1=\Theta_2-\frac{2\pi}{3}+2n\pi$, $\Theta_3=\Theta_2+\frac{2\pi}{3}+2n'\pi$, where n and n' are integers. We also define the reduced hyperangle $\theta_i\equiv\arctan\frac{2|R_i|}{\sqrt{3}|s_i|}$, $\theta_i\in[0,\frac{\pi}{2}]$. Three fermions in 1D have six different sorting orders. If $x_1<x_2<x_3$, the 111 expansion is simplified as

$$\begin{aligned}\Psi={}&\frac{2}{3\sqrt{3}}B^3\cos(3\theta_2)-2a_pB^2\cos(2\theta_2)+2\sqrt{3}a_p^2B\cos\theta_2-\frac{3}{4}\left(2a_p^3+a_p^2r_p\right)\\&-\frac{D_F}{\pi B^3}\cos(3\theta_2)-\frac{3\sqrt{3}D_Fa_p}{\pi B^4}\cos(4\theta_2)-\frac{18D_Fa_p^2}{\pi B^5}\cos(5\theta_2)-\frac{45\sqrt{3}D_F}{4\pi B^6}\left(2a_p^3+a_p^2r_p\right)\cos(6\theta_2)\\&-\frac{405D_Fa_p^3r_p}{2\pi B^7}\cos(7\theta_2)-\frac{945\sqrt{3}D_F}{16\pi B^8}\left(6a_p^3r_p^2+a_p^2r_p'\right)\cos(8\theta_2)+O(B^{-9}).\end{aligned} \tag{21}$$

Our resultant 21 expansion is

$$\begin{aligned}\Psi={}&\Bigg[-R^2+3a_p|R|-\frac{3}{4}\left(2a_p^2+a_pr_p\right)+\frac{3\sqrt{3}D_F}{2\pi R^4}+\frac{9\sqrt{3}a_pD_F}{\pi|R|^5}+\frac{45\sqrt{3}D_F}{4\pi R^6}\left(2a_p^2+a_pr_p\right)\\&+\frac{405\sqrt{3}D_F}{4\pi|R|^7}a_p^2r_p+\frac{945\sqrt{3}D_F}{32\pi R^8}\left(6a_p^2r_p^2+a_pr_p'\right)\Bigg]\phi(s)\\&+\left[-\frac{3}{2}+\frac{45\sqrt{3}D_F}{2\pi R^6}+\frac{405\sqrt{3}a_pD_F}{2\pi|R|^7}+\frac{2835\sqrt{3}D_F}{8\pi R^8}\left(2a_p^2+a_pr_p\right)\right]f(s)+\frac{2835\sqrt{3}D_F}{4\pi R^8}g(s)+O(R^{-9}).\end{aligned} \tag{22}$$

We need to emphasize that Eq. (22) is applicable when the interaction does not support any two-body bound states. If the interaction supports n_b two-body bound states, three fermions may form such a two-body bound state and a free fermion, which fly apart with total kinetic energy equal to the released two-body binding energy. In this case, the 21 expansion is modified as [22]

$$\Psi = \Psi_{21} + \sum_{n=1}^{n_b} c_n\phi_n(s)\exp\left(i\frac{2}{\sqrt{3}}\kappa_n|R|\right), \tag{23}$$

where Ψ_{21} is defined as the right-hand side of Eq. (22). The second term on the right-hand side of Eq. (23) is the outgoing wave with wave number $2\kappa_n/\sqrt{3} > 0$. Here ϕ_n is the wave function of the nth two-body p-wave bound state with energy $E_n = -\hbar^2\kappa_n^2/m$ and satisfies the Schrödinger equation and the normalization condition:

$$\left(-\frac{d^2}{ds^2} + \frac{mV(s)}{\hbar^2} + \kappa_n^2\right)\phi_n(s) = 0, \tag{24}$$

$$\int_{-\infty}^{\infty} ds|\phi_n(s)|^2 = 1. \tag{25}$$

The coefficients c_n are in general nonuniversal parameters that depend on the details of the interaction potentials. c_n determines the probability amplitude of producing the nth bound state which fly apart from the remaining fermion after the three-body zero-energy collision. But using probability conservation, one can show that these coefficients are related to the imaginary part of the three-body scattering hypervolume. As the outgoing wave contributes a positive probability flux towards the outside of a large circle centered at the origin in the plane of coordinates $(\frac{\sqrt{3}}{2}s, R)$, D_F gains a negative imaginary part to make the total flux through the circle vanish and conserve the probability. From this conservation of probability we derive the relation between the imaginary part of D_F and the norm-squares of the coefficients c_n:

$$\mathrm{Im}D_F = -\frac{3\sqrt{3}}{2}\sum_{n=1}^{n_b}\kappa_n|c_n|^2. \tag{26}$$

Even if $n_b = 1$, one can*not* determine c_1 completely from $\mathrm{Im}D_F$, because the phase of c_1 cannot be determined from $\mathrm{Im}D_F$. To determine c_n, one need to solve the three-body Schrödinger equation using the actual interaction potentials between the fermions.

In Sec. VI we will study the relation between $\mathrm{Im}D_F$ and the three-body recombination rates of one-dimensional ultracold spin-polarized Fermi gases.

IV. EVALUATION OF THE SCATTERING HYPERVOLUME FOR SEVERAL INTERACTION POTENTIALS

In this section, we first derive an approximate formula for the hypervolume D_F for weak potentials by using the Born expansion. We then numerically compute D_F for the square-barrier and the square-well pairwise potentials and the Gaussian pairwise potentials having various strengths.

A. Weak interaction potentials

If the potentials $V(s)$ and $U(s_1, s_2, s_3)$ are weak, we can express the wave function as a Born expansion [22,29]:

$$\Psi = \Psi_0 + \Psi_1 + \Psi_2 + \cdots, \tag{27}$$

where $\Psi_0 = s_1s_2s_3 = s^3/4 - sR^2$ is the wave function of three free fermions, $\Psi_n = (\widehat{G}\mathcal{V})^n\Psi_0$, $\widehat{G} = -\widehat{H}_0^{-1}$ is the Green's operator, $\widehat{H}_0$ is the three-body kinetic-energy operator, and $\mathcal{V} = U(s_1, s_2, s_3) + \sum_i V(s_i)$ is the interaction potential.

We derive the first-order and the second-order corrections at $|s_i| \gg r_e$:

$$\Psi_1 = -\frac{3\sqrt{3}s_1s_2s_3}{4\pi B^6}\Lambda - \sum_{i=1}^{3}\left(\alpha_1B^2\cos 2\Theta_i + \frac{\alpha_3}{2}\right)\mathrm{sgn}(s_i) + O(UB^{-9}), \tag{28a}$$

$$\Psi_2 = \sum_{i=1}^{3}\left[\beta_1B^2\cos 2\Theta_i - \frac{6\alpha_1^2}{\pi}R_i\theta_i + \beta_3\right]\mathrm{sgn}(s_i) - \frac{3\sqrt{3}s_1s_2s_3}{20\pi B^6}(25\alpha_3^2 - 7\alpha_1\alpha_5) + O(V^2B^{-9}) + O(UV) + O(U^2), \tag{28b}$$

where

$$\alpha_n = \frac{m}{\hbar^2}\int_0^\infty ds\, s^{n+1}V(s), \tag{29a}$$

$$\beta_1 = \frac{m^2}{\hbar^4}\int_0^\infty ds\int_0^s ds'\, 2ss'^2V(s)V(s'), \tag{29b}$$

$$\beta_3 = \frac{m^2}{\hbar^4}\int_0^\infty ds\int_0^s ds'\, (ss'^4 + 2s^3s'^2)V(s)V(s'), \tag{29c}$$

$$\Lambda = \frac{m}{\hbar^2}\int_{-\infty}^\infty ds'\int_{-\infty}^\infty dR'\left(\frac{1}{4}s'^3 - s'R'^2\right)^2U(s', R'). \tag{29d}$$

See Appendix A for details of the derivation.

By comparing the results in Eqs. (28) with the 111 expansion in Eq. (19), we find the expansions of a_p and D_F in powers of the interaction potential:

$$a_p = \alpha_1 - \beta_1 + O(V^3), \tag{30}$$

$$D_F = \frac{\Lambda}{2} + \frac{1}{10}(25\alpha_3^2 - 7\alpha_1\alpha_5) + O(V^3) + O(UV) + O(U^2). \tag{31}$$

For any particular two-body potential $V(s)$, e.g., the square-well potential or the Gaussian potential, one can calculate a_p by solving the two-body Schrödinger equation and verify that the result is consistent with Eq. (30) if V is weak. Equation (31) shows that D_F is quadratically dependent on the two-body potential V if V is weak, and the three-body potential U is absent. On the other hand, D_F is linearly dependent on U if U is weak.

If the interactions are not weak, one can solve the three-body Schrödinger equation numerically at zero energy and match the resultant wave function with the asymptotic expansions in Eqs. (19) and (23) to numerically extract the value of D_F.

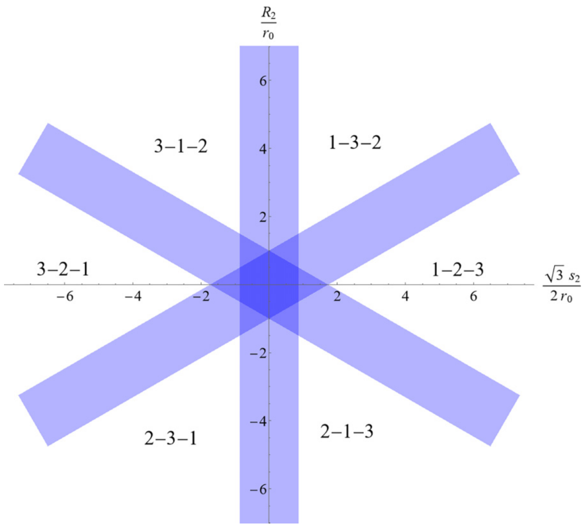

FIG. 2. The possible configurations of three particles in one dimension. The potential vanishes outside of the colored belts. The whole plane can be divided into six regions corresponding to six different orders of the coordinates of the three particles. The corresponding order of the three particles is labeled in each region in the figure.

B. Numerical computations

The three-body problem in 1D for zero total momentum is equivalent to a one-body problem on a 2D plane. The three-body wave function Ψ here depends only on (s, R) or (B, Θ), where $s \equiv s_2$, $R \equiv R_2$, and $\Theta \equiv \Theta_2$. We define the two-dimensional vector $\mathbf{B} = (\frac{\sqrt{3}}{2}s, R)$, and $\Psi = \Psi(\mathbf{B})$. The zero-energy Schrödinger equation is

$$-\nabla^2\Psi + \frac{4m}{3\hbar^2}\mathcal{V}\Psi = 0, \tag{32}$$

where ∇^2 is the Laplace operator in 2D:

$$\nabla^2 = \frac{1}{B}\frac{\partial}{\partial B}\left(B\frac{\partial}{\partial B}\right) + \frac{1}{B^2}\frac{\partial^2}{\partial\Theta^2}. \tag{33}$$

Because the interaction potential conserves parity and Ψ_0 has odd parity, we can assume that Ψ has odd parity, namely,

$$\Psi(-x_1, -x_2, -x_3) = -\Psi(x_1, x_2, x_3). \tag{34}$$

From the above equation and the Fermi statistics we can show that

$$\Psi(B, -\Theta) = \Psi(B, \Theta) \tag{35}$$

and

$$\Psi\left(B, \Theta + \frac{\pi}{3}\right) = -\Psi(B, \Theta). \tag{36}$$

We can divide the 2D plane into six regions; see Fig. 2. Each region corresponds to a specific order of the coordinates of the three fermions, and we only need to solve Eq. (32) in one of the six regions. In the remainder of this section, we always choose to solve the problem in the region $-\pi/6 < \Theta < \pi/6$ which corresponds to the order of the coordinates $x_1 < x_2 < x_3$.

According to Eqs. (35) and (36), the wave function can be expanded as the following Fourier series:

$$\Psi(B, \Theta) = \sum_{i=1}^{\infty}\frac{1}{\sqrt{B}}f_i(B)\cos{(6i-3)\Theta}. \tag{37}$$

The potential $\mathcal{V}$ can also be expanded as

$$\frac{m}{\hbar^2}\mathcal{V}(B, \Theta) = \frac{v_0(B)}{2} + \sum_{i=1}^{\infty}v_{6i}(B)\cos 6i\Theta. \tag{38}$$

The Schrödinger equation (32) can be written as coupled ordinary differential equations:

$$-f'' + \mathcal{U}f = 0, \tag{39}$$

where $f = (f_1, f_2, f_3, \dots)^{\mathrm{T}}$ is a column vector, f'' means d^2f/dB^2, and $\mathcal{U} = \mathcal{U}(B)$ is a symmetric matrix dependent on B. The matrix elements of U are

$$\mathcal{U}_{ii} = \frac{(6i-3)^2 - 1/4}{B^2} + \frac{2}{3}(v_0 + v_{12i-6}), \tag{40a}$$

$$\mathcal{U}_{ij} = \frac{2}{3}(v_{6|i-j|} + v_{6(i+j-1)}) \text{ if } i \neq j. \tag{40b}$$

Given the wave function on a circle with radius B centered at the origin in the $(\frac{\sqrt{3}}{2}s_2, R_2)$ plane, one can use the Schrödinger equation to uniquely determine the wave function inside such a circle, and therefore determine the partial derivative of the wave function with respect to B on the circle. Therefore the partial derivative of the wave function with respect to B on such a circle depends linearly on the wave function on such a circle. So there is a matrix F such that

$$f' = Ff. \tag{41}$$

Substituting the above equation into Eq. (39), and requiring that Eq. (39) be satisfied for all f, we find that F satisfies a first-order differential equation:

$$F' = \mathcal{U} - F^2. \tag{42}$$

At small B, we can solve Eq. (39) to find the analytical solution to f_i (for square well potentials) or find an expansion of f_i in powers of B (for other potentials); from these we can analytically determine F at infinitesimal B and see that it is diagonal. Using the result of F at infinitesimal B as our initial condition, we then solve Eq. (42) numerically and determine F at $B = B_0$ for some large B_0. Matching Eq. (41) at $B = B_0$ with the 111 and the 21 expansions of Ψ, we can approximately determine D_F. We then compare the approximate values of D_F determined in this way by using various large values of B_0. We approximately extrapolate to the $B_0 \to \infty$ limit to find the value of D_F with some numerical uncertainty.

1. Square-barrier and square-well potentials

For the square-barrier or square-well potential with strength V_0 (V_0 can be positive or negative),

$$V(s) = V_0\frac{\hbar^2}{mr_0^2} \times \begin{cases} 1, & |s| < r_0 \\ 0, & |s| > r_0. \end{cases} \tag{43}$$

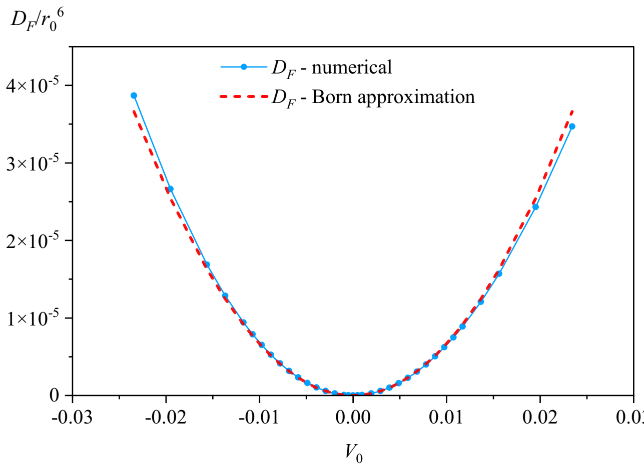

FIG. 3. D_F for weak square-barrier or square-well potentials. The blue solid line shows the numerical results and the red dashed line shows the Born approximation.

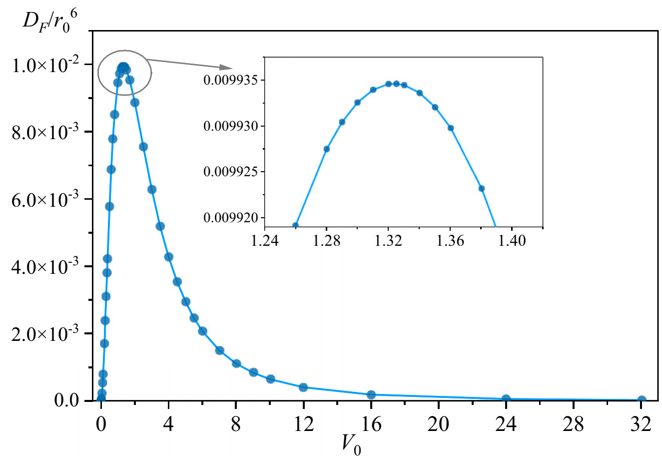

FIG. 4. The value of D_F for the repulsive square-barrier potential defined in Eq. (43).

We can analytically calculate all the Fourier components of $\mathcal{V}$:

$$\nu_0 = \frac{V_0}{r_0^2} \times \begin{cases} 6, & 0 \leqslant B \leqslant \frac{\sqrt{3}}{2} r_0 \\ \frac{12}{\pi}\theta_0, & \frac{\sqrt{3}}{2} r_0 < B, \end{cases} \tag{44}$$

$$\nu_{6i} = \frac{V_0}{r_0^2} \times \begin{cases} 0, & 0 \leqslant B \leqslant \frac{\sqrt{3}}{2} r_0 \\ (-1)^i \frac{12}{\pi} \frac{\sin 6i\theta_0}{6i}, & \frac{\sqrt{3}}{2} r_0 < B, \end{cases} \tag{45}$$

for $i \geqslant 1$, where $\theta_0 = \arcsin(\sqrt{3} r_0/2B)$.

In the region $B \leqslant \sqrt{3} r_0/2$, the potential $\mathcal{V} = 3V_0\hbar^2/mr_0^2$ is a constant, and $\nu_0 = 6V_0/r_0^2$, $\nu_{6i} = 0$ for $i \geqslant 1$. So $\mathcal{U}$ is diagonal in this region and f can be analytically determined:

$$f_i = \begin{cases} c_i \sqrt{B} I_{6i-3}(2\sqrt{V_0}B/r_0), & V_0 > 0 \\ c_i' \sqrt{B} J_{6i-3}(2\sqrt{-V_0}B/r_0), & V_0 < 0, \end{cases} \tag{46}$$

where I_j is the modified Bessel function of the first kind, and J_j is the Bessel function of the first kind.

At $0 < B \leqslant \sqrt{3} r_0/2$, F is diagonal and its elements can be easily calculated by using Eq. (46). Equation (42) is a first-order ordinary differential equation, and the initial value of F at $B = \sqrt{3} r_0/2$ is known, so we can compute F numerically at any $B > \sqrt{3} r_0/2$. At large B, we use the 111 and the 21 expansions of the wave function in Eqs. (19) and (23) to determine $f_1, f_2, f_3, \dots$ approximately. By solving Eq. (41), we get the numerical value of the scattering hypervolume D_F. Figure 3 shows our results of D_F at small V_0. According to Eq. (29a) we have

$$\alpha_n = \frac{V_0}{n+2} r_0^n. \tag{47}$$

If V_0 is small, by using Eq. (31) we get

$$D_F = \tfrac{1}{15} V_0^2 r_0^6 + O(V_0^3). \tag{48}$$

The blue solid line in Fig. 3 shows the numerical results and the red dashed line corresponds to the Born approximation $D_F \simeq \frac{1}{15} V_0^2 r_0^6$. The numerical results agree quite well with the Born approximation for small values of V_0.

Figure 4 shows the full curve of D_F for repulsive V_0. D_F increases at $0 < V_0 < V_c$ where $V_c \simeq 1.325$. At $V_0 = V_c$, D_F has a maximum of about $0.0099 r_0^6$. D_F decreases at $V_0 > V_c$. In the following we prove that D_F approaches zero as $V_0 \to +\infty$ and scales as $1/V_0^3$ at large V_0 for the square-barrier potentials.

If $V_0 = +\infty$, the square-barrier potential becomes the hard-core potential. In this case, the wave function goes to zero in the blue banded region in Fig. 2. We use the new coordinates $\mathbf{B}' = (\frac{\sqrt{3}}{2}(s - 2r_0), R)$. $\Psi(\mathbf{B}) \equiv \widetilde{\Psi}(\mathbf{B}')$ satisfies the Laplace equation in the sector area, and $\widetilde{\Psi}(\mathbf{B}')$ satisfies the following boundary conditions:

$$\widetilde{\Psi}\left(B', \Theta' = -\frac{\pi}{6}\right) = \widetilde{\Psi}\left(B', \Theta' = \frac{\pi}{6}\right) = 0, \tag{49}$$

where B', Θ' are defined via $\frac{\sqrt{3}}{2}(s - 2r_0) = B' \cos\Theta'$, $R = B' \sin\Theta'$. In the domain $-\pi/6 < \Theta' < \pi/6$, one can easily find the analytical solution:

$$\widetilde{\Psi}(\mathbf{B}') = \frac{2}{3\sqrt{3}} B'^3 \cos 3\Theta'. \tag{50}$$

If we change back to the coordinates $\mathbf{B} = (\frac{\sqrt{3}}{2}s, R)$, we get

$$\Psi = \frac{2}{3\sqrt{3}} B^3 \cos 3\theta_2 - 2B^2 r_0 \cos 2\theta_2 + 2\sqrt{3} B r_0^2 \cos\theta_2 - 2r_0^3. \tag{51}$$

Note that, at $V_0 = +\infty$, Eq. (51) is the exact solution and is not just the asymptotic expansion of Ψ. On the other hand, the 111 expansion in this area is simplified as Eq. (21). For the hard-core potential with $r_0 = 1$, we have $a_p = r_0$, $r_p = 2r_0/3$. One can check that Eq. (51) agrees with Eq. (21) if $D_F = 0$. So $D_F = 0$ for the hard-core potential, and this is consistent with our numerical results for the values of D_F for the square-barrier potential at $V_0 \to \infty$.

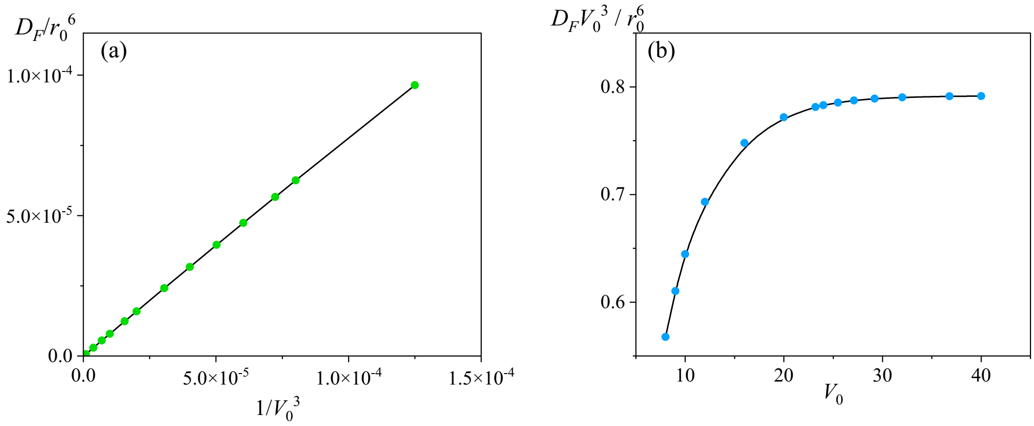

FIG. 5. (a) D_F vs $1/V_0^3$ for the repulsive square-barrier potentials. (b) $D_F V_0^3$ vs V_0 for these potentials. The subfigures (a) and (b) both show that D_F is proportional to $1/V_0^3$ if V_0 is large.

If V_0 is large but finite, we also get an expansion in powers of $1/V_0$:

$$\begin{aligned}\widetilde{\Psi}(\mathbf{B}') &= \frac{2}{3\sqrt{3}}B'^3\cos 3\theta' + \frac{2}{\sqrt{V_0}}B'^2\cos 2\theta' + \frac{2\sqrt{3}}{V_0}B'\cos\theta' + \frac{9}{4V_0^{3/2}} + O(B'^{-3})\\ &= \frac{2}{3\sqrt{3}}B^3\cos 3\theta_2 - 2B^2\cos 2\theta_2\left(1-\frac{1}{\sqrt{V_0}}\right) + 2\sqrt{3}B\cos\theta_2\left(1-\frac{1}{\sqrt{V_0}}\right)^2\\ &\quad -\left(2-\frac{6}{\sqrt{V_0}}+\frac{6}{V_0}-\frac{9}{4V_0^{3/2}}\right) + O(B^{-3}).\end{aligned} \tag{52}$$

If $1/\sqrt{V_0} \ll B' \ll r_0$, the wave function $\widetilde{\Psi}(\mathbf{B}')$ satisfies a scaling law: if $\widetilde{\Psi}(\mathbf{B}')$ is the solution at interaction strength V_0, then $\widetilde{\Psi}(\sqrt{\lambda}\mathbf{B}')$ is the solution at interaction strength λV_0. According to this we know the next term in the first line of Eq. (52) should take the form $1/V_0^3 B'^3$, which implies that D_F scales as V_0^{-3} at large V_0:

$$D_F = \frac{\mathcal{C}}{V_0^3} + o\big(V_0^{-3}\big). \tag{53}$$

Figure 5 shows that our numerical results agree with this. From the numerical results we get $\mathcal{C} \simeq 0.79$.

2. Gaussian potential

In this section we consider the Gaussian potential

$$V(s) = V_0\frac{\hbar^2}{mr_0^2}e^{-s^2/r_0^2}, \tag{54}$$

where the strength V_0 can be positive or negative. According to Eq. (29a) we get

$$\alpha_n = \frac{1}{2}\Gamma\left(1+\frac{n}{2}\right)V_0 r_0^n. \tag{55}$$

If V_0 is small, by using Eq. (31) we get the Born approximation of D_F:

$$D_F = \frac{3\pi}{16}V_0^2 r_0^6 + O\big(V_0^3\big). \tag{56}$$

To numerically compute the value of D_F, we also Fourier-expand the wave function and the potential function. The Fourier components of $\mathcal{V}$ for the Gaussian potential can be calculated analytically:

$$v_{6i}(B) = (-1)^i\frac{6V_0}{r_0^2}I_{3i}\left(\frac{2B^2}{3r_0^2}\right)e^{-2B^2/3r_0^2}, \tag{57}$$

where $i = 0, 1, 2, \ldots$. At small B, unlike the case of a square-well potential, we cannot get an analytical expression for the matrix F for the Gaussian potential. However we can solve Eq. (39) to find an expansion of f_i in powers of B, and get an approximate expression for the matrix F at small B. The remaining algorithm is similar to the case of square-well potential, and we get the numerical values of D_F for the repulsive and the attractive Gaussian potentials.

Figure 6 shows our numerical results of D_F at small V_0. We see that the results are consistent with the Born approximation.

Figure 7 shows the values of D_F for repulsive Gaussian potentials. D_F/r_0^6 has a maximum of about 0.144 at $V_0 \simeq 1.91$. D_F/r_0^6 decreases at $V_0 > 1.91$. The rate of the decrease is slower than in the case of square-well potentials.

Figure 8 shows our results of D_F for attractive Gaussian potentials. If the potential strength is weak, there is no two-body bound state. As the depth of the potential increases, two-body bound states appear one by one. At $V_0 = V_{c1} \simeq -2.684$ the first p-wave resonance occurs, and the first two-body bound state appears. When V_0 is close to V_{c1} we find an approximate formula for a_p/r_0:

$$a_p/r_0 \simeq -3.007/(V_0 - V_{c1}) + 1.041. \tag{58}$$

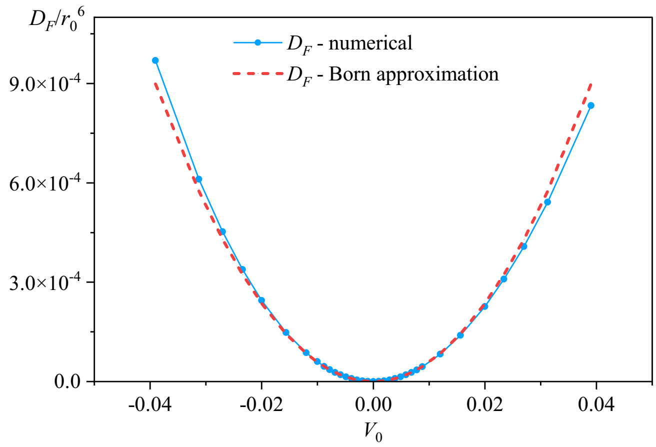

FIG. 6. The values of D_F for weak Gaussian potentials. The blue solid line shows the numerical results and the red dashed line shows the Born approximation.

At $V_0 = V_{c2} \simeq -17.796$, the second p-wave resonance occurs, and the second two-body bound state appears. These resonances are indicated by the vertical black dot-dashed lines in Fig. 8. At $V_{c1} < V_0 < 0$ there is no two-body bound state and D_F is real. When V_0 approaches V_{c1} from above, D_F diverges. To understand the behavior of D_F when V_0 is close to V_{c1}, we plot $\ln(D_F/r_0^6)$ vs $\ln(V_0 - V_{c1})$ when V_0 is slightly greater than V_{c1}, in Fig. 9(a). It seems that there is a linear relationship. Doing a linear fit, we find that D_F is proportional to $(V_0 - V_{c1})^{-6}$, and we derive an approximate formula: $D_F \simeq 0.74a_p^6$ when V_0 is slightly greater than V_{c1}.

At $V_{c2} < V_0 < V_{c1}$ there is one two-body p-wave bound state, and in this case D_F gains a negative imaginary part, $D_F = \mathrm{Re}D_F + i\mathrm{Im}D_F$. The absolute value of $\mathrm{Im}D_F$ is smaller than the absolute value of $\mathrm{Re}D_F$ for most values of V_0 in this range. When V_0 approaches V_{c1} from below, $\mathrm{Re}D_F$ and $\mathrm{Im}D_F$ both diverge. We plot $\ln[\mathrm{Re}(D_F/r_0^6)]$ and $\ln[-\mathrm{Im}(D_F/r_0^6)]$ vs $\ln(V_{c1} - V_0)$ when V_0 is slightly less than V_{c1}, in Fig. 9(b). We again see approximately linear relationships. Doing linear fits, we find that $\mathrm{Re}D_F$ seems to be proportional to $(V_{c1} - V_0)^{-5}$ but $\mathrm{Im}D_F$ is perhaps proportional to $(V_{c1} - V_0)^{-6}$, and we get an approximate formula: $\mathrm{Im}D_F \simeq -0.46a_p^6$ when V_0 is slightly less than V_{c1}. According to the results in Sec. VI, the divergence of $\mathrm{Im}D_F$ indicates that a one-dimensional spin-polarized Fermi gas will suffer strong three-body recombination losses near such resonances.

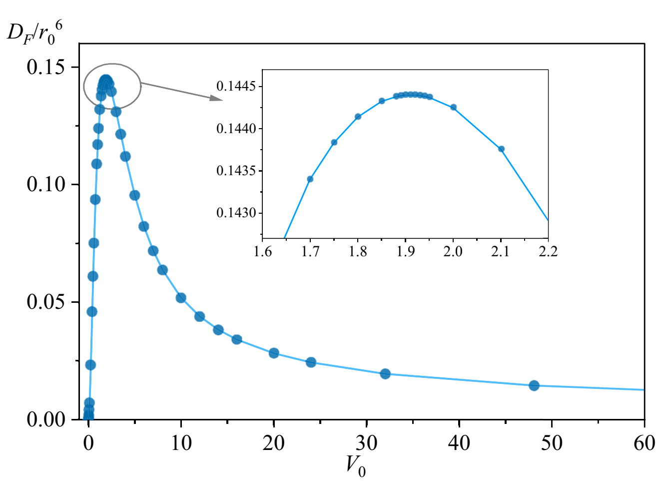

FIG. 7. The values of D_F for repulsive Gaussian potentials.

If V_0 is slightly less than V_{c1}, a_p is positive and very large, and the two-body bound state is very shallow. The energy of the shallow bound state satisfies the universal formula:

$$E_2 \simeq -\hbar^2/ma_p^2. \tag{59}$$

According to the Bose-Fermi duality [32,33], the properties of the one-dimensional Fermi system with large and positive scattering length are similar to those of a weakly attractive bosonic system, which can be described by using the Lieb-Liniger model [34] with the repulsive contact interaction replaced by attractive contact interaction, and this model can be exactly solved by using the Bethe ansatz [35]. Reference [36] shows that such a bosonic system has a three-body bound state with energy $E_3 = 4E_2$. Mapping this bosonic system to the fermionic system with two-body p-wave scattering length $a_p \gg r_0$, we infer a three-body bound state with energy

$$E_3 \simeq -4\hbar^2/ma_p^2. \tag{60}$$

When V_0 is slightly less than V_{c1}, we indeed find that a three-body bound state appears. We have numerically solved the Schrödinger equation to find the energies of the two-body and the three-body bound states with Gaussian pairwise interactions. These energies are plotted in Fig. 10. We find that when V_0 is less than but close to V_{c1}, these bound-state energies are indeed close to the predictions of the aforementioned universal formulas.

The one-dimensional square-barrier and square-well potentials and the Gaussian potential we have studied above are different from the true interactions of ultracold atoms in quasi-one-dimensional (quasi-1D) optical waveguides in which the transverse motion of the atoms is frozen to a length scale $a_\perp$ that is usually much larger than the characteristic range of the van der Waals potential between the atoms. The 1D effective range r_p of ultracold atoms in quasi-1D is much larger than the range of atomic interaction [37], but the model potentials we have studied above have $r_p \sim r_0$. In Ref. [38] it is shown that the large 1D effective range has important consequences for the three-body states, and in particular the ratio between the energies of the three-body shallow bound state and the two-body shallow bound state deviates significantly from four at large and positive a_p [38], in contrast to Eqs. (59) and (60) in our paper. Therefore the effect of the large 1D effective range on the three-body scattering hypervolume D_F may also be large for real ultracold atoms. The numerical calculation of D_F for real ultracold atoms is expected to be much more difficult than the numerical calculations in this paper: one would need to solve the three-body Schrödinger equation in three dimensions. We leave this as an open question.

V. ENERGY SHIFTS DUE TO D_F

We consider three identical spin-polarized fermions on a line with length L and impose the periodic boundary condition on the wave function: $\Psi(x_1 + L, x_2, x_3) = \Psi(x_1, x_2, x_3)$. Consider an energy eigenstate in which the momenta of the

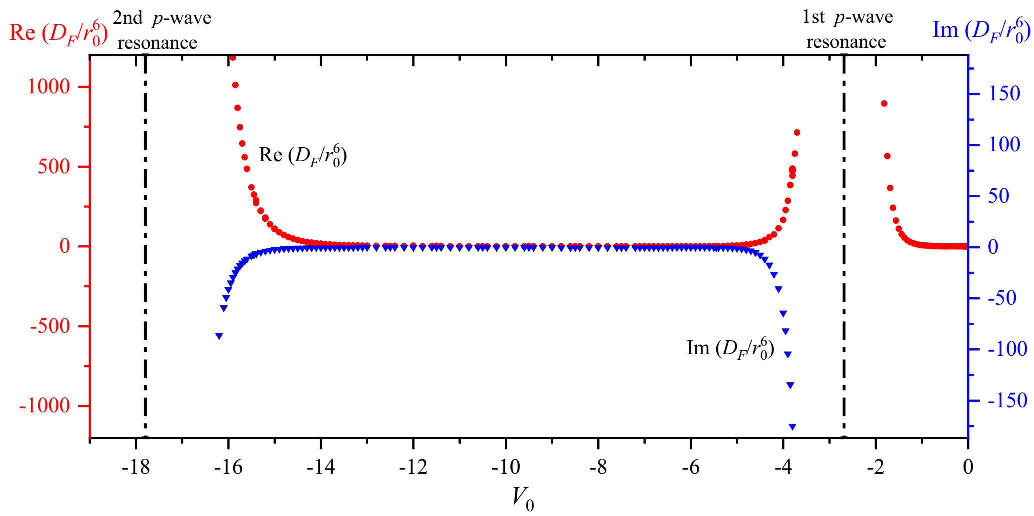

FIG. 8. The values of D_F for attractive Gaussian potentials. The red dots represent the real part of D_F/r_0^6 and the blue triangles represent the imaginary part of D_F/r_0^6. The vertical dashed lines show the critical strengths of the Gaussian potential at which the p-wave resonances occur.

fermions are k_1, k_2, and k_3 in the absence of interactions. When we introduce interactions that give rise to a nonzero D_F, the shift of the energy eigenvalue due to a nonzero D_F is

$$\mathcal{E}_{k_1k_2k_3} = \frac{\hbar^2 D_F}{12mL^2}(k_1-k_2)^2(k_2-k_3)^2(k_3-k_1)^2. \quad (61)$$

See Appendix B for the details of the derivation of this formula.

In addition, if there are two-body interactions, in general the shift of the energy of the three fermions will also contain terms due to the two-body parameters including a_p, r_p, etc.; nevertheless, the shift due to D_F in Eq. (61) is still valid. We can also calculate the leading-order shift of the three-body energy due to a_p by using a method similar to the one used in Appendix B:

$$\mathcal{E}^{\text{2-body}}_{k_1k_2k_3} = \frac{\hbar^2 a_p}{mL}[(k_1-k_2)^2+(k_2-k_3)^2+(k_3-k_1)^2]. \quad (62)$$

We then generalize the energy shift to N fermions in the periodic length L. The number density of the fermions is $n = N/L$. We define the Fermi wave number $k_F = \pi n$, the Fermi energy $\epsilon_F = \hbar^2 k_F^2/2m$, and the Fermi temperature $T_F = \epsilon_F/k_B$, where k_B is the Boltzmann constant.

A. Adiabatic shifts of energy and pressure in the thermodynamic limit due to D_F

Starting from a many-body state at a finite temperature T, if we introduce a nonzero D_F *adiabatically*, the energy shift to first order in D_F is equal to the sum of the contributions from

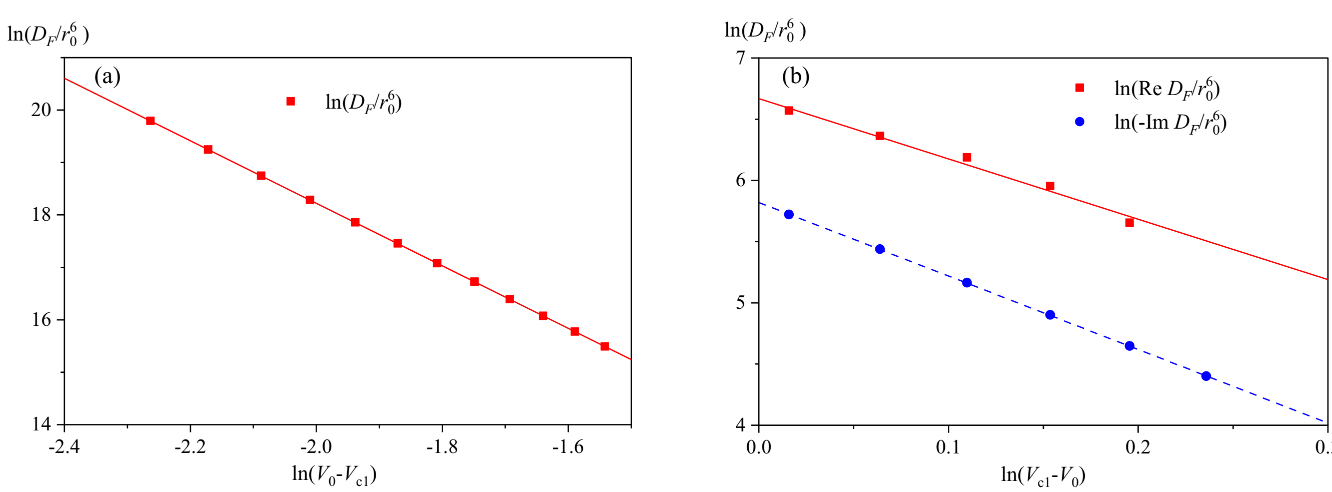

FIG. 9. (a) $\ln(D_F/r_0^6)$ vs $\ln(V_0 - V_{c1})$ when V_0 is slightly greater than V_{c1}. Doing a linear fit in this double-log plot, we find that $D_F \simeq 542.9 r_0^6/(V_0 - V_{c1})^{5.963\pm0.002} \simeq 0.74 a_p^6$. (b) $\ln[\text{Re}(D_F/r_0^6)]$ (red squares) and $\ln[-\text{Im}(D_F/r_0^6)]$ (blue dots) plotted against $\ln(V_{c1} - V_0)$ when V_0 is slightly less than V_{c1}. Doing linear fits in these double-log plots, we find that $\text{Re}D_F \simeq 796 r_0^6/(V_{c1} - V_0)^{4.98\pm0.36}$ and $\text{Im}D_F \simeq -337 r_0^6/(V_{c1} - V_0)^{6.00\pm0.02} \simeq -0.46 a_p^6$, where we have used the approximate formula Eq. (58).

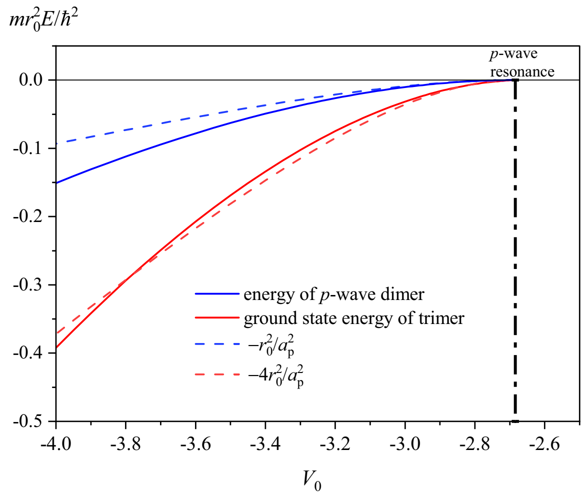

FIG. 10. The energies of bound states with Gaussian pairwise interactions vs the interaction strength V_0. The blue solid line shows the two-body bound-state energy, and the red solid line shows the three-body bound-state energy. The dashed lines correspond to the universal formulas in Eqs. (59) and (60).

all the triples of fermions, namely,

$$\Delta E = \frac{1}{6}\sum_{k_1k_2k_3} \mathcal{E}_{k_1k_2k_3} n_{k_1} n_{k_2} n_{k_3}, \tag{63}$$

where $n_k = (e^{\beta(\epsilon_k-\mu)}+1)^{-1}$ is the Fermi-Dirac distribution function, $\beta = 1/k_BT$, $\epsilon_k = \hbar^2k^2/2m$ is the kinetic energy of a fermion, and μ is the chemical potential. The summation over k can be replaced by a continuous integral $\sum_k = L\int dk/(2\pi)$ in the thermodynamic limit. Carrying out the integral, we get

$$\Delta E(T) = \frac{N\hbar^2 D_F}{768\sqrt{\pi}m} k_F^8 \times \widetilde{T}^{9/2}\left[3f_{1/2}(z)f_{3/2}(z)f_{5/2}(z) - f_{3/2}^3(z)\right], \tag{64}$$

where $\widetilde{T} = T/T_F$, $z = e^{\beta\mu}$, and the function $f_\nu(z)$ is defined as

$$f_\nu(z) \equiv -\mathrm{Li}_\nu(-z) = \frac{2}{\Gamma(\nu)}\int_0^\infty dx \frac{x^{2\nu-1}}{1+e^{x^2}/z}, \tag{65}$$

where Li_ν is the polylogarithm function. The number of fermions satisfies

$$N = \sum_k \frac{1}{e^{\beta(\epsilon_k-\mu)}+1},$$

and this leads to the equation of the chemical potential μ:

$$\frac{2}{\sqrt{\pi}} = \sqrt{\widetilde{T}} f_{1/2}(e^{\widetilde{\mu}/\widetilde{T}}), \tag{66}$$

where $\widetilde{\mu} = \mu/\epsilon_F$.

In the low-temperature limit, namely, $T \ll T_F$,

$$\Delta E(T) = \frac{N\hbar^2 D_F}{405\pi^2 m} k_F^8\left[1 + \frac{3}{2}\pi^2\widetilde{T}^2 + O(\widetilde{T}^4)\right]. \tag{67}$$

In an intermediate temperature regime, $T_F \ll T \ll T_e$,

$$\Delta E(T) = \frac{N\hbar^2 D_F}{48\pi^2 m} k_F^8 \widetilde{T}^3\left[1 + \frac{9}{4\sqrt{2\pi\widetilde{T}}} + O(\widetilde{T}^{-1})\right], \tag{68}$$

where $T_e = \hbar^2/2mr_e^2k_B$. If T is comparable to or higher than T_e, the de Broglie wavelengths of the fermions will be comparable to or shorter than the range r_e of interparticle interaction potentials, and we can no longer use the effective parameter D_F to describe the system. See Fig. 11(a) for ΔE as a function of the initial temperature.

The pressure of the spin-polarized Fermi gas changes by the following amount due to the adiabatic introduction of D_F:

$$\Delta p = -\left(\frac{\partial \Delta E}{\partial L}\right)_{S,N} = \frac{8\Delta E}{L}, \tag{69}$$

where the subscripts S, N prescribe that we keep the entropy S and the particle number N fixed when taking the partial derivative. See Fig. 11(b) for Δp as a function of the initial temperature.

B. Isothermal shifts of energy and pressure in the thermodynamic limit due to D_F

If the interaction is introduced adiabatically, the temperature will increase (if $D_F > 0$) or decrease (if $D_F < 0$). The change of temperature is

$$\Delta T = \left(\frac{\partial \Delta E}{\partial S}\right)_{N,L}. \tag{70}$$

So if we introduce D_F isothermally, the energy shift $\Delta E'$ should be

$$\Delta E' = \Delta E - C\Delta T = \left(1 - T\frac{\partial}{\partial T}\right)\Delta E, \tag{71}$$

where C is the heat capacity of the noninteracting Fermi gas at constant volume. In the low-temperature limit $T \ll T_F$,

$$\Delta E'(T) = \frac{N\hbar^2 D_F k_F^8}{405\pi^2 m}\left[1 - \frac{3}{2}\pi^2\widetilde{T}^2 + O(\widetilde{T}^4)\right]. \tag{72}$$

In an intermediate-temperature regime $T_F \ll T \ll T_e$,

$$\Delta E'(T) = \frac{N\hbar^2 D_F}{48\pi^2 m} k_F^8 \widetilde{T}^3\left[-2 - \frac{27}{8\sqrt{2\pi\widetilde{T}}} + O(\widetilde{T}^{-1})\right]. \tag{73}$$

According to Eqs. (72) and (73), $\Delta E'$ changes sign as we increase the temperature. Therefore, there is a critical temperature T_c at which $\Delta E' = 0$. We find

$$T_c \simeq 0.2268 T_F. \tag{74}$$

The pressure of the spin-polarized Fermi gas changes by the following amount due to the isothermal introduction of D_F:

$$\Delta p' = \Delta p - \frac{2C\Delta T}{L} = \left(1 - \frac{1}{4}T\frac{\partial}{\partial T}\right)\Delta p. \tag{75}$$

In the low-temperature limit $T \ll T_F$,

$$\Delta p' = \frac{8n\hbar^2 D_F}{405\pi^2 m} k_F^8\left[1 + \frac{3}{4}\pi^2\widetilde{T}^2 + O(\widetilde{T}^4)\right]. \tag{76}$$

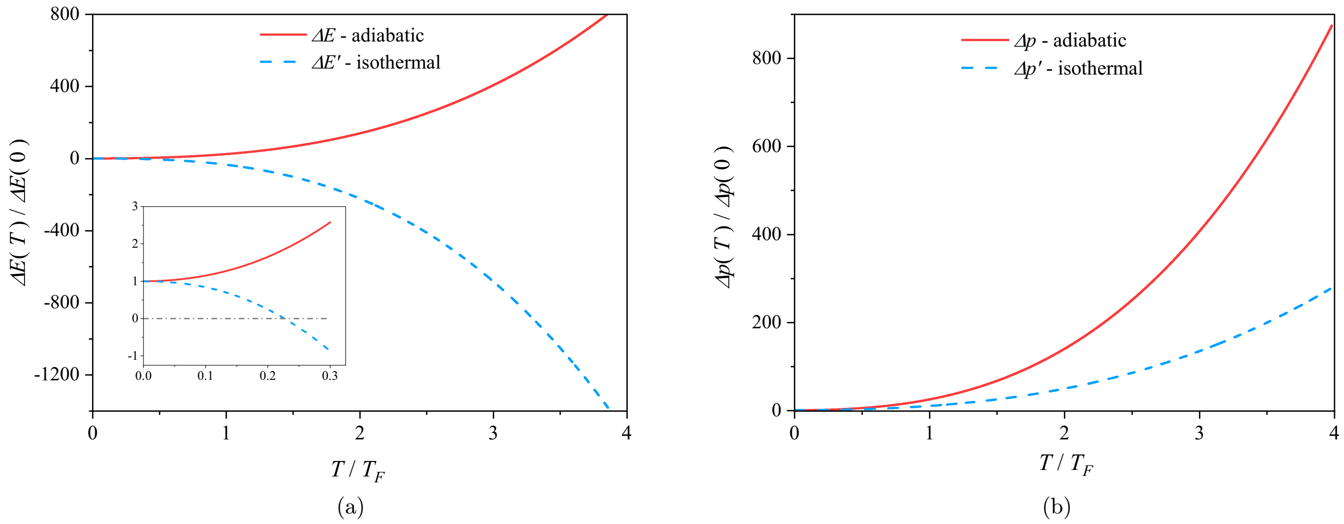

FIG. 11. The shifts of (a) energy and (b) pressure caused by the adiabatic (red solid lines) or isothermal (blue dashed lines) introduction of D_F vs the temperature T. At $T \simeq 0.2268 T_F$, the isothermal energy shift ΔE changes sign.

In an intermediate-temperature regime $T_F \ll T \ll T_e$,

$$\Delta p' = \frac{n\hbar^2 D_F}{6\pi^2 m} k_F^8 \widetilde{T}^3 \left[\frac{1}{4} + \frac{27}{32\sqrt{2\pi\widetilde{T}}} + O(\widetilde{T}^{-1})\right]. \quad (77)$$

The shifts of energy and pressure are plotted as functions of temperature in Figs. 11(a) and 11(b), respectively.

VI. THE THREE-BODY RECOMBINATION RATE

If the collision of the three particles is purely elastic, D_F is a real number. But if the two-body interaction supports bound states, then the three-body collisions are usually not purely elastic, and the three-body recombination may occur. In this case, D_F becomes complex, and the three-body recombination rate constant is proportional to the imaginary part of D_F [22,39].

Within a short time Δt, the probability that no recombination occurs is $\exp(-2|\mathrm{Im}E|\Delta t/\hbar) \simeq 1 - 2|\mathrm{Im}E|\Delta t/\hbar$. Then the probability for one recombination is $2|\mathrm{Im}E|\Delta t/\hbar$. Since each recombination event causes the loss of three low-energy fermions, the change of the number of remaining low-energy fermions in the short time dt is

$$dN = -\frac{1}{6}\sum_{k_1k_2k_3} 3\frac{2dt}{\hbar}|\mathrm{Im}\mathcal{E}_{k_1k_2k_3}|n_{k_1}n_{k_2}n_{k_3}. \quad (78)$$

This leads to

$$\frac{dn}{dt} = -L_3 n^3, \quad (79)$$

and the coefficient L_3 is

$$L_3 = \frac{\pi^{3/2}}{128}\frac{\hbar|\mathrm{Im}D_F|}{m}k_F^6 \times \widetilde{T}^{9/2}\left[3f_{1/2}(z)f_{3/2}(z)f_{5/2}(z) - f_{3/2}^3(z)\right]. \quad (80)$$

L_3 depends on the density n and the temperature T.

In the low-temperature limit $T \ll T_F$,

$$L_3 \simeq \frac{2}{135}\left(1 + \frac{3\pi^2}{2}\widetilde{T}^2\right)\frac{\hbar|\mathrm{Im}D_F|}{m}k_F^6. \quad (81)$$

In particular, at $T = 0$,

$$L_3 = \frac{2\hbar|\mathrm{Im}D_F|}{135m}k_F^6, \quad (82)$$

and L_3 is proportional to n^6.

In an intermediate-temperature regime $T_F \ll T \ll T_e$, we find that

$$L_3 \simeq \frac{m^2}{\hbar^5}|\mathrm{Im}D_F|(k_B T)^3, \quad (83)$$

and L_3 is approximately proportional to T^3, which is consistent with the prediction in Ref. [14].

VII. SUMMARY AND DISCUSSION

We derived the asymptotic expansions of the three-body wave function Ψ for identical spin-polarized fermions colliding at zero energy in one dimension and defined the three-body scattering hypervolume D_F. Now the scattering hypervolumes of spin-polarized fermions have been defined in 3D [28], 2D [29], and 1D. For weak interaction potentials, we derived an approximate formula for D_F by using the Born expansion. For stronger interactions, one can solve the three-body Schrödinger equation numerically at zero energy and match the resultant wave function with the asymptotic expansion formulas we have derived in this paper to numerically compute the values of D_F. We did such numerical calculations for the square-barrier, square-well, and Gaussian potentials.

We considered three fermions along a line with periodic boundary condition and derived the shifts of their energy eigenvalues due to a nonzero D_F and then considered the dilute spin-polarized Fermi gas in 1D and derived the shifts of its energy and pressure due to a nonzero D_F.

Finally, we studied the dilute spin-polarized atomic Fermi gas in 1D with interaction potentials that support two-body bound states, for which we have three-body recombination processes and D_F has nonzero imaginary part, and we derived formulas for the three-body recombination rate constant L_3 in terms of the imaginary part of D_F and the temperature and density of the Fermi gas.

One can similarly define the three-body scattering hypervolumes for identical bosons or for distinguishable particles in 1D and study their physical implications.

For ultracold atoms, one can use the optical lattice to confine them in quasi-1D, and the van der Waals range of the interatomic potential is usually much shorter than the radial confinement length. One can solve the three-body problem in three-dimensional space to numerically determine the one-dimensional scattering hypervolume of the three atoms.

ACKNOWLEDGMENT

This work was supported by the National Key R&D Program of China (Grants No. 2019YFA0308403 and No. 2021YFA1400902).

APPENDIX A: BORN SERIES FOR WEAK INTERACTIONS

For weak interaction potentials, we can expand the wave function as a Born series:

$$\Psi = \Psi_0 + \widehat{G}\mathcal{V}\Psi_0 + (\widehat{G}\mathcal{V})^2\Psi_0 + \cdots, \tag{A1}$$

where $\Psi_0 = s_1 s_2 s_3 = s^3/4 - sR^2$ is the wave function of three free fermions, $\widehat{G} = -\widehat{H}_0^{-1}$ is the Green's operator, $\widehat{H}_0$ is the three-body kinetic-energy operator. $\mathcal{V} = U(s_1, s_2, s_3) + \sum_i V(s_i)$, where $V(s_i)$ and U are two-body and three-body finite-range potentials whose characteristic range is r_e.

1. The first-order term

The first-order term Ψ_1 in the Born series is

$$\begin{aligned}\Psi_1 &= \widehat{G}\mathcal{V}\Psi_0 = \widehat{G}U\Psi_0 + \sum_i \widehat{G}V_i\Psi_0\\ &= \frac{m}{\hbar^2}\int d^2\boldsymbol{\xi}'\mathcal{G}(\boldsymbol{\xi}-\boldsymbol{\xi}')U(\boldsymbol{\xi}')\Psi_0(\boldsymbol{\xi}')\\ &\quad + \frac{m}{\hbar^2}\sum_i\int d^2\boldsymbol{\xi}'\mathcal{G}(\boldsymbol{\xi}-\boldsymbol{\xi}')V_i(\boldsymbol{\xi}')\Psi_0(\boldsymbol{\xi}'),\end{aligned} \tag{A2}$$

where $\boldsymbol{\xi} = (s, 2R/\sqrt{3})$ and $\boldsymbol{\xi}' = (s', 2R'/\sqrt{3})$ are two-dimensional vectors, and $V_i(\boldsymbol{\xi}') = V(s_i')$. Without losing generality, we set $s_2' = s'$, $s_1' = -\frac{1}{2}s' + R'$, $s_3' = -\frac{1}{2}s' - R'$. $\mathcal{G}$ is the Green's function [22,29] in two-dimensional space which satisfies $\nabla_{\xi}^2\mathcal{G}(\boldsymbol{\xi}-\boldsymbol{\xi}') = \delta(\boldsymbol{\xi}-\boldsymbol{\xi}')$, and its expression is

$$\mathcal{G}(\boldsymbol{\xi}-\boldsymbol{\xi}') = \frac{1}{2\pi}\ln|\boldsymbol{\xi}-\boldsymbol{\xi}'|. \tag{A3}$$

We define

$$\Psi_{1i} \equiv \widehat{G}V_i\Psi_0. \tag{A4}$$

For $i = 2$, we have $V_i(\boldsymbol{\xi}') = V(s')$ and

$$\begin{aligned}\Psi_{1i} &= \frac{m}{\hbar^2}\int d^2\boldsymbol{\xi}'\mathcal{G}(\boldsymbol{\xi}-\boldsymbol{\xi}')V_i(\boldsymbol{\xi}')\Psi_0(\boldsymbol{\xi}')\\ &= \frac{m}{\hbar^2}\int_{-\infty}^{\infty}dx'\int_{-\infty}^{\infty}dy'\frac{1}{16\pi}\ln[(x_i-x')^2+(y_i-y')^2]\\ &\quad\times V(x')(x'^3-3x'y'^2).\end{aligned} \tag{A5}$$

Here and in the following, we define $x_i = s_i$, $x' = s'$, $y_i = 2R_i/\sqrt{3}$, and $y' = 2R'/\sqrt{3}$ for simplicity. We first integrate over y' in Eq. (A5). To avoid the divergence in the integral, we integrate over y' from $-\lambda$ to λ first and then take the limit $\lambda \to \infty$. Then we integrate over x' and take the sum over i to get

$$\begin{aligned}\sum_i \Psi_{1i} = \sum_i\bigg[&-\frac{1}{2}\alpha_3(x_i) + \frac{3}{4}\alpha_1(x_i)\big(y_i^2 - x_i^2\big)\\ &-x_i\bar{\alpha}_2(x_i) - \frac{1}{4}\big(x_i^3 - 3x_i y_i^2\big)\bar{\alpha}_0(x_i)\bigg],\end{aligned} \tag{A6}$$

where the functions $\alpha_n(x)$ and $\bar{\alpha}_n(x)$ at $x > 0$ are defined as

$$\alpha_n(x) = \frac{m}{\hbar^2}\int_0^x dx'\, x'^{n+1}V(x'), \tag{A7a}$$

$$\bar{\alpha}_n(x) = \frac{m}{\hbar^2}\int_x^{\infty} dx' x'^{n+1}V(x'). \tag{A7b}$$

At $x > r_e$, $\alpha_n(x)$ becomes a constant α_n and $\bar{\alpha}_n(x) = 0$ because the potential $V(x')$ vanishes at $x' > r_e$. We also require $\alpha_n(x)$ to be odd functions and $\bar{\alpha}_n(x)$ to be even functions of x, namely,

$$\alpha_n(-x) = -\alpha_n(x), \quad \bar{\alpha}_n(-x) = \bar{\alpha}_n(x). \tag{A8}$$

If $|x_1|$, $|x_2|$, and $|x_3|$ are all greater than r_e, Eq. (A6) is simplified as

$$\sum_i \Psi_{1i} = \sum_i\left[-\frac{1}{2}\alpha_3 + \frac{3}{4}\alpha_1\big(y_i^2 - x_i^2\big)\right]\mathrm{sgn}(x_i). \tag{A9}$$

For any values of x_i,

$$\begin{aligned}\widehat{G}U\Psi_0 &= \frac{m}{\hbar^2}\int_{-\infty}^{\infty}dx'\int_{-\infty}^{\infty}dy'\frac{1}{16\pi}\ln[(x_i-x')^2+(y_i-y')^2]\\ &\quad\times U(x',y')(x'^3-3x'y'^2).\end{aligned} \tag{A10}$$

Since U is a finite-range potential, the integral on the right-hand side of Eq. (A10) may be expanded when x_i and y_i go to infinity simultaneously. Expanding this integral at large B, we get

$$\begin{aligned}\widehat{G}U\Psi_0 &\simeq \frac{m}{\hbar^2}\frac{-\big(x^3-3xy^2\big)}{24\pi(x^2+y^2)^3}\int_{-\infty}^{\infty}dx'\int_{-\infty}^{\infty}dy'U(x',y')\\ &\quad\times\,(x'^3-3x'y'^2)^2\\ &= -\frac{m}{\hbar^2}\frac{3\sqrt{3}s_1s_2s_3}{4\pi B^6}\int_{-\infty}^{\infty}ds'\int_{-\infty}^{\infty}dR'U(s',R')(s_1's_2's_3')^2\\ &\equiv -\frac{3\sqrt{3}s_1s_2s_3}{4\pi B^6}\Lambda.\end{aligned} \tag{A11}$$

2. The second-order term

The second-order term Ψ_2 in the Born series is

$$\begin{aligned}\Psi_2 &= \widehat{G}\mathcal{V}\Psi_1\\ &= \sum_{ij}\widehat{G}V_i\widehat{G}V_j\Psi_0 + \sum_i \widehat{G}V_i\widehat{G}U\Psi_0 + \sum_i \widehat{G}U\widehat{G}V_i\Psi_0 + (\widehat{G}U)^2\Psi_0.\end{aligned} \tag{A12}$$

We define

$$\begin{aligned}\Psi_{2,ij} &= \widehat{G}V_i\widehat{G}V_j\Psi_0\\ &= \frac{m}{\hbar^2}\iint dx'dy'\frac{1}{4\pi}\ln[(x_i-x')^2+(y_i-y')^2]V(x')\Psi_{1j}(x',y').\end{aligned} \tag{A13}$$

In particular, if $j=i$,

$$\Psi_{2,ii} = \iint dx'dy'\frac{1}{4\pi}\ln\big[(x_i-x')^2+(y_i-y')^2\big]V(x')\Big[-\frac{1}{2}\alpha_3(x')+\frac{3}{4}\alpha_1(x')(y'^2-x'^2)-\bar{\alpha}_2(x')x'-\frac{1}{4}(x'^3-3x'y'^2)\bar{\alpha}_0(x')\Big]. \tag{A14}$$

If $|x_1|$, $|x_2|$, and $|x_3|$ are all greater than r_e, we can evaluate the integral to obtain

$$\Psi_{2,ii} = \Big[\beta_3 - \frac{3}{4}\big(y_i^2-x_i^2\big)\beta_1\Big]\mathrm{sgn}(x_i), \tag{A15}$$

where β_1 and β_3 are defined as

$$\beta_1 = \int_0^\infty dx\int_0^x dx'\, 2xx'^2V(x)V(x'), \tag{A16a}$$

$$\beta_3 = \int_0^\infty dx\int_0^x dx'\,(xx'^4+2x^3x'^2)V(x)V(x'). \tag{A16b}$$

If $j\neq i$,

$$\begin{aligned}\sum_{j\neq i}\Psi_{2,ij} = \frac{1}{4\pi}\iint dx'dy'\ln[(x_i-x')^2+(y_i-y')^2]V(x')\Big[&-\frac{1}{2}\alpha_3(x_2')+\frac{3}{4}\alpha_3(x_2')\big(y_2'^2-x_2'^2\big)-x_2'\bar{\alpha}_2(x_2')\\ &-\frac{1}{4}\big(x_2'^3-3x_2'y_2'^2\big)\bar{\alpha}_0(x_2')-\frac{1}{2}\alpha_3(x_3')+\frac{3}{4}\alpha_3(x_3')\big(y_3'^2-x_3'^2\big)-x_2'\bar{\alpha}_2(x_3')-\frac{1}{4}\big(x_3'^3-3x_3'y_3'^2\big)\bar{\alpha}_0(x_3')\Big],\end{aligned} \tag{A17}$$

where $x_2'=-\frac{1}{2}x'+\frac{\sqrt{3}}{2}y'$, $y_2'=-\frac{\sqrt{3}}{2}x'-\frac{1}{2}y'$, $x_3'=-\frac{1}{2}x'-\frac{\sqrt{3}}{2}y'$, $y_3'=+\frac{\sqrt{3}}{2}x'-\frac{1}{2}y'$.

$$\begin{aligned}\sum_{j\neq i}\Psi_{2,ij} = &\frac{1}{4\pi}\iint dx'dy'V(x')\left[\frac{1}{2}\alpha_3\left(\frac{\sqrt{3}}{2}y'\right)-\alpha_1\left(\frac{\sqrt{3}}{2}y'\right)\left(x'^2-\frac{3}{8}y'^2\right)+\frac{\sqrt{3}}{2}y'\bar{\alpha}_2\left(\frac{\sqrt{3}}{2}y'\right)-\frac{\sqrt{3}}{2}x'^2y'\bar{\alpha}_0\left(\frac{\sqrt{3}}{2}y'\right)\right]\\ &\times\left\{\ln\left[(x_i-x')^2+\left(y_i-y'+\frac{1}{\sqrt{3}}x'\right)^2\right]-\ln\left[(x_i-x')^2+\left(y_i-y'-\frac{1}{\sqrt{3}}x'\right)^2\right]\right\}\\ &+\frac{1}{4\pi}\iint dx'dy'V(x')\left[\frac{\sqrt{3}}{2}x'y'\alpha_1\left(\frac{\sqrt{3}}{2}y'\right)+\frac{3}{4}x'y'^2\bar{\alpha}_0\left(\frac{\sqrt{3}}{2}y'\right)\right]\\ &\times\left\{\ln\left[(x_i-x')^2+\left(y_i-y'+\frac{1}{\sqrt{3}}x'\right)^2\right]+\ln\left[(x_i-x')^2+\left(y_i-y'-\frac{1}{\sqrt{3}}x'\right)^2\right]\right\}.\end{aligned} \tag{A18}$$

We define

$$\begin{aligned}&\frac{1}{2}\alpha_3\left(\frac{\sqrt{3}}{2}y'\right)-\alpha_1\left(\frac{\sqrt{3}}{2}y'\right)\left(x'^2-\frac{3}{8}y'^2\right)+\frac{\sqrt{3}}{2}y'\bar{\alpha}_2\left(\frac{\sqrt{3}}{2}y'\right)-\frac{\sqrt{3}}{2}x'^2y'\bar{\alpha}_0\left(\frac{\sqrt{3}}{2}y'\right)\\ &\quad\equiv\frac{1}{2}\alpha_3\mathrm{sgn}(y')-\alpha_1\left(x'^2-\frac{3}{8}y'^2\right)\mathrm{sgn}(y')+f_1(x',y'),\end{aligned} \tag{A19}$$

where

$$f_1(x',y') = f_{11}(y')+x'^2f_{12}(y'), \tag{A20}$$

and

$$f_{11}(y')=\frac{1}{2}\alpha_3\left(\frac{\sqrt{3}}{2}y'\right)-\frac{1}{2}\alpha_3\mathrm{sgn}(y')+\frac{3}{8}y'^2\alpha_1\left(\frac{\sqrt{3}}{2}y'\right)-\frac{3}{8}y'^2\alpha_1\mathrm{sgn}(y')+\frac{\sqrt{3}}{2}y'\bar{\alpha}_2\left(\frac{\sqrt{3}}{2}y'\right), \tag{A21}$$

$$f_{12}(y')=-\alpha_1\left(\frac{\sqrt{3}}{2}y'\right)+\alpha_1\mathrm{sgn}(y')-\frac{\sqrt{3}}{2}y'\bar{\alpha}_0\left(\frac{\sqrt{3}}{2}y'\right). \tag{A22}$$

f_{11} and f_{12} are odd functions of y'. They are short-range functions, namely, they vanish at $\sqrt{3}|y'|/2>r_e$.

We also define

$$\frac{\sqrt{3}}{2}x'y'\alpha_1\left(\frac{\sqrt{3}}{2}y'\right)+\frac{3}{4}x'y'^2\bar{\alpha}_0\left(\frac{\sqrt{3}}{2}y'\right)\equiv\frac{\sqrt{3}}{2}\alpha_1x'y'\mathrm{sgn}(y')+x'f_2(y'), \tag{A23}$$

$$f_2(y')=\frac{\sqrt{3}}{2}y'\alpha_1\left(\frac{\sqrt{3}}{2}y'\right)+\frac{3}{4}y'^2\bar{\alpha}_0\left(\frac{\sqrt{3}}{2}y'\right)-\frac{\sqrt{3}}{2}y'\alpha_1. \tag{A24}$$

f_2 is an even function of y'. It vanishes at $\sqrt{3}|y'|/2>r_e$. Then

$$\begin{aligned}\sum_{j\neq i}\Psi_{2,ij}=&\frac{1}{4\pi}\iint dx'dy'V(x')\left[\frac{1}{2}\alpha_3\mathrm{sgn}(y')-\alpha_1\left(x'^2-\frac{3}{8}y'^2\right)\mathrm{sgn}(y')+f_{11}(y')+x'^2f_{12}(y')\right]\\&\times\left\{\ln\left[(x_i-x')^2+\left(y_i-y'+\frac{1}{\sqrt{3}}x'\right)^2\right]-\ln\left[(x_i-x')^2+\left(y_i-y'-\frac{1}{\sqrt{3}}x'\right)^2\right]\right\}\\&+\frac{1}{4\pi}\iint dx'dy'V(x')\left[\frac{\sqrt{3}}{2}\alpha_1x'y'\mathrm{sgn}(y')+x'f_2(y')\right]\\&\times\left\{\ln\left[(x_i-x')^2+\left(y_i-y'+\frac{1}{\sqrt{3}}x'\right)^2\right]+\ln\left[(x_i-x')^2+\left(y_i-y'-\frac{1}{\sqrt{3}}x'\right)^2\right]\right\}.\end{aligned} \tag{A25}$$

For large x_i and y_i, we get

$$\begin{aligned}\sum_{j\neq i}\Psi_{2,ij}=&-\frac{3\sqrt{3}}{\pi}\alpha_1^2y_i\theta_i\mathrm{sgn}(x_i)-\frac{\left(x_i^3-3x_iy_i^2\right)}{\sqrt{3}\pi\left(x_i^2+y_i^2\right)^3}\left(\frac{20}{9}\alpha_3^2-\frac{28}{45}\alpha_1\alpha_5\right)\\&+(\text{terms which will cancel after summation over } i)+O(B^{-4}).\end{aligned} \tag{A26}$$

We have not evaluated the terms $\widehat{G}V_i\widehat{G}U\Psi_0$, $\widehat{G}U\widehat{G}V_i\Psi_0$ and $(\widehat{G}U)^2\Psi_0$ in the Born series. The full expression of Ψ_2 is

$$\begin{aligned}\Psi_2=&\sum_i\left[\beta_3-\frac{3}{4}\left(y_i^2-x_i^2\right)\beta_1-\frac{3\sqrt{3}}{\pi}\alpha_1^2y_i\theta_i\right]\mathrm{sgn}(x_i)-\frac{\left(x^3-3xy^2\right)}{\sqrt{3}\pi(x^2+y^2)^3}\left(\frac{20}{3}\alpha_3^2-\frac{28}{15}\alpha_1\alpha_5\right)+O(V^2B^{-9})\\&+O(UV)+O(U^2),\end{aligned} \tag{A27}$$

as is shown in the main text.

Comparing the resultant Born series and the 111 expansion of the wave function, we get

$$a_p=\alpha_1-\beta_1+O(V^3), \tag{A28a}$$

$$a_p^2r_p=-\frac{2}{3}\alpha_3+\frac{4}{3}\beta_3+O(V^3), \tag{A28b}$$

and

$$\begin{aligned}D_F=&\frac{\Lambda}{2}+\frac{5}{2}\alpha_3^2-\frac{7}{10}\alpha_1\alpha_5+O(V^3)\\&+O(UV)+O(U^2).\end{aligned} \tag{A29}$$

For the square-well potential with strength V_0 and range $r_e=1$,

$$\alpha_1=\tfrac{1}{3}V_0,\quad \alpha_3=\tfrac{1}{5}V_0,\quad \alpha_5=\tfrac{1}{7}V_0, \tag{A30a}$$

$$\beta_1=\tfrac{2}{15}V_0^2,\quad \beta_3=\tfrac{13}{105}V_0^2. \tag{A30b}$$

Substituting these results, we get

$$a_p=\tfrac{1}{3}V_0-\tfrac{2}{15}V_0^2+O\left(V_0^3\right), \tag{A31a}$$

$$a_p^2r_p=-\tfrac{2}{15}V_0+\tfrac{52}{315}V_0^2+O\left(V_0^3\right), \tag{A31b}$$

which are consistent with the direct calculation of a_p and r_p. For the scattering hypervolume, we have

$$D_F=\tfrac{1}{15}V_0^2+O\left(V_0^3\right), \tag{A32}$$

which is consistent with the result of numerical computations for small V_0.

APPENDIX B: SHIFTS OF THE ENERGY OF THREE FERMIONS IN ONE DIMENSION WITH PERIODIC BOUNDARY CONDITIONS DUE TO D_F

The normalized wave function of three free fermions with momenta $\hbar k_1, \hbar k_2, \hbar k_3$ in a large periodic line with length L is

$$\Psi_{k_1k_2k_3} = \frac{1}{\sqrt{6}L^{3/2}}\begin{vmatrix} e^{ik_1x_1} & e^{ik_1x_2} & e^{ik_1x_3} \\ e^{ik_2x_1} & e^{ik_2x_2} & e^{ik_2x_3} \\ e^{ik_3x_1} & e^{ik_3x_2} & e^{ik_3x_3}\end{vmatrix}. \tag{B1}$$

We define the Jacobi momenta $\hbar q$, $\hbar p$, $\hbar k_c$ such that

$$k_1 = \tfrac{1}{3}k_c + \tfrac{1}{2}q + p, \tag{B2a}$$

$$k_2 = \tfrac{1}{3}k_c + \tfrac{1}{2}q - p, \tag{B2b}$$

$$k_3 = \tfrac{1}{3}k_c - q. \tag{B2c}$$

$\hbar k_c$ is the total momentum of three fermions. We extract the motion of the center of mass $R_c = (x_1 + x_2 + x_3)/3$,

$$\Psi_{k_1k_2k_3} = \frac{1}{\sqrt{L}}e^{ik_c\cdot R_c}\Phi_{p,q}. \tag{B3}$$

Suppose that the typical momentum of each fermion is $\approx 2\pi\hbar/\lambda$. For small hyperradii, $B \ll \lambda$, we Taylor expand $\Phi_{p,q}$ and get

$$\Phi_{p,q} \simeq \frac{-i}{\sqrt{6}L}\left(p^3 - \frac{9}{4}pq^2\right)\left(\frac{1}{4}s^3 - sR^2\right). \tag{B4}$$

$\Phi_{p,q}$ is the wave function of the relative motion of three free fermions. If we introduce a small three-body D_F adiabatically, $\Phi_{p,q}$ is changed to

$$\Phi_{p,q} \simeq \frac{-i}{\sqrt{6}L}\left(p^3 - \frac{9}{4}pq^2\right)\left(\frac{1}{4}s^3 - sR^2\right)\left(1 - \frac{3\sqrt{3}D_F}{2\pi B^6}\right) \tag{B5}$$

for $r_e \ll B \ll \lambda$. The wave function satisfies the free Schrödinger equation outside of the range of interaction,

$$-\frac{\hbar^2}{m}\nabla_{\boldsymbol{\xi}}^2\Phi_{p,q} = E\Phi_{p,q}, \tag{B6}$$

where $\boldsymbol{\xi} = (s, 2R/\sqrt{3})$ is a two-dimensional vector, E is the energy of the relative motion, and $B = \sqrt{3}\xi/2$.

For large values of L, we may compute the energy E approximately. We rewrite Eq. (B6) as

$$-\frac{\hbar^2}{m}\nabla_{\boldsymbol{\xi}}^2\Phi_1 = E_1\Phi_1, \tag{B7a}$$

$$-\frac{\hbar^2}{m}\nabla_{\boldsymbol{\xi}}^2\Phi_2^* = E_2\Phi_2^*, \tag{B7b}$$

for two slightly different interactions that yield two slightly different scattering hypervolumes, D_{F1} and D_{F2} respectively. Here we omit the subscript p, q for simplicity. Multiplying both sides of Eq. (B7a) by Φ_2^*, multiplying both sides of Eq. (B7b) by Φ_1, subtracting the two resultant equations, and taking the two-dimensional integral over $\boldsymbol{\xi}$ for $\xi > \xi_0$ (where ξ_0 is any length scale satisfying $r_e \ll \xi_0 \ll \lambda$), we get

$$-\frac{\hbar^2}{m}\int_{\xi>\xi_0} d^2\xi\,\nabla_{\boldsymbol{\xi}}\cdot(\Phi_2^*\nabla_{\boldsymbol{\xi}}\Phi_1 - \Phi_1\nabla_{\boldsymbol{\xi}}\Phi_2^*) = (E_1 - E_2)\int_{\xi>\xi_0} d^2\xi\,\Phi_1\Phi_2^*. \tag{B8}$$

In the bulk part of the configuration space, $\Phi_1 \simeq \Phi_2$. Note also that the wave function for the relative motion is normalized, and that the volume of the region $\xi < \xi_0$ is small and may be omitted in the normalization integral. So the right-hand side of Eq. (B8) is

$$\frac{2}{\sqrt{3}}(E_1 - E_2)\int_{\xi>\xi_0} dsdR|\Phi|^2 \simeq \frac{2}{\sqrt{3}}(E_1 - E_2). \tag{B9}$$

Applying Gauss's theorem to the left-hand side of Eq. (B8), we get

$$-\frac{\hbar^2}{m}\oint_{\xi=\xi_0} d\mathbf{S}\cdot(\Phi_2^*\nabla_{\boldsymbol{\xi}}\Phi_1 - \Phi_1\nabla_{\boldsymbol{\xi}}\Phi_2^*) \simeq \frac{2}{\sqrt{3}}(E_1 - E_2), \tag{B10}$$

where S is the surface of the circle with radius $\xi = \xi_0$ centered at the origin, and $d\mathbf{S}$ points toward the center of the circle.

To evaluate the integral on the circle $\xi = \xi_0$, we parametrize $\boldsymbol{\xi} = (\xi^{(1)}, \xi^{(2)})$ as

$$\xi^{(1)} = \xi\cos\varphi, \tag{B11a}$$

$$\xi^{(2)} = \xi\sin\varphi, \tag{B11b}$$

where $0 \leqslant \varphi < 2\pi$. Here $\xi^{(1)} = s$ and $\xi^{(2)} = 2R/\sqrt{3}$. The surface element $d\mathbf{S}$ is

$$d\mathbf{S} = -\boldsymbol{\xi}d\varphi. \tag{B12}$$

The minus sign in the above equation means that the direction of $d\mathbf{S}$ is towards the origin. Assuming that Φ_1 and Φ_2 satisfy Eq. (B5) with $D_F = D_{F1}$ and $D_F = D_{F2}$, respectively, and evaluating the integral in Eq. (B10) on the circle with radius $\xi = \xi_0$, we get

$$\begin{aligned} E_1 - E_2 &= \frac{\hbar^2}{3mL^2}(D_{F1} - D_{F2})\left(p^3 - \frac{9}{4}pq^2\right)^2 \\ &= \frac{\hbar^2}{12mL^2}(D_{F1} - D_{F2})(k_1 - k_2)^2(k_2 - k_3)^2 \\ &\quad\times (k_3 - k_1)^2. \end{aligned} \tag{B13}$$

This result agrees with Eq. (61) in the main text.

[1] A. Görlitz, J. M. Vogels, A. E. Leanhardt, C. Raman, T. L. Gustavson, J. R. Abo-Shaeer, A. P. Chikkatur, S. Gupta, S. Inouye, T. Rosenband, and W. Ketterle, Realization of Bose-Einstein Condensates in Lower Dimensions, Phys. Rev. Lett. **87**, 130402 (2001).

[2] F. Schreck, L. Khaykovich, K. L. Corwin, G. Ferrari, T. Bourdel, J. Cubizolles, and C. Salomon, Quasipure Bose-Einstein Condensate Immersed in a Fermi Sea, Phys. Rev. Lett. **87**, 080403 (2001).

[3] S. Dettmer, D. Hellweg, P. Ryytty, J. J. Arlt, W. Ertmer, K. Sengstock, D. S. Petrov, G. V. Shlyapnikov, H. Kreutzmann, L. Santos, and M. Lewenstein, Observation of Phase Fluctuations in Elongated Bose-Einstein Condensates, Phys. Rev. Lett. **87**, 160406 (2001).

[4] M. Greiner, I. Bloch, O. Mandel, T. W. Hänsch, and T. Esslinger, Exploring Phase Coherence in a 2D Lattice of Bose-Einstein Condensates, Phys. Rev. Lett. **87**, 160405 (2001).

[5] H. Moritz, T. Stöferle, M. Köhl, and T. Esslinger, Exciting Collective Oscillations in a Trapped 1D Gas, Phys. Rev. Lett. **91**, 250402 (2003).

[6] B. Paredes, A. Widera, V. Murg, O. Mandel, S. Fölling, I. Cirac, G. V. Shlyapnikov, T. W. Hänsch, and I. Bloch, Tonks–Girardeau gas of ultracold atoms in an optical lattice, Nature (London) **429**, 277 (2004).

[7] T. Kinoshita, T. Wenger, and D. S. Weiss, Observation of a one-dimensional Tonks-Girardeau gas, Science **305**, 1125 (2004).

[8] N. Syassen, D. M. Bauer, M. Lettner, T. Volz, D. Dietze, J. J. García-Ripoll, J. I. Cirac, G. Rempe, and S. Dürr, Strong dissipation inhibits losses and induces correlations in cold molecular gases, Science **320**, 1329 (2008).

[9] E. Haller, M. Gustavsson, M. J. Mark, J. G. Danzl, R. Hart, G. Pupillo, and H.-C. Nägerl, Realization of an excited, strongly correlated quantum gas phase, Science **325**, 1224 (2009).

[10] E. Haller, M. J. Mark, R. Hart, J. G. Danzl, L. Reichsöllner, V. Melezhik, P. Schmelcher, and H.-C. Nägerl, Confinement-Induced Resonances in Low-Dimensional Quantum Systems, Phys. Rev. Lett. **104**, 153203 (2010).

[11] M. A. Cazalilla, R. Citro, T. Giamarchi, E. Orignac, and M. Rigol, One dimensional bosons: From condensed matter systems to ultracold gases, Rev. Mod. Phys. **83**, 1405 (2011).

[12] X.-W. Guan, M. T. Batchelor, and C. Lee, Fermi gases in one dimension: From Bethe ansatz to experiments, Rev. Mod. Phys. **85**, 1633 (2013).

[13] N. P. Mehta and J. R. Shepard, Three bosons in one dimension with short-range interactions: Zero-range potentials, Phys. Rev. A **72**, 032728 (2005).

[14] N. P. Mehta, B. D. Esry, and C. H. Greene, Three-body recombination in one dimension, Phys. Rev. A **76**, 022711 (2007).

[15] Y. Nishida, Universal bound states of one-dimensional bosons with two- and three-body attractions, Phys. Rev. A **97**, 061603(R) (2018).

[16] L. Pricoupenko, Pure confinement-induced trimer in one-dimensional atomic waveguides, Phys. Rev. A **97**, 061604(R) (2018).

[17] G. Guijarro, A. Pricoupenko, G. E. Astrakharchik, J. Boronat, and D. S. Petrov, One-dimensional three-boson problem with two- and three-body interactions, Phys. Rev. A **97**, 061605(R) (2018).

[18] Y. Sekino and Y. Nishida, Quantum droplet of one-dimensional bosons with a three-body attraction, Phys. Rev. A **97**, 011602(R) (2018).

[19] M. Valiente, Three-body repulsive forces among identical bosons in one dimension, Phys. Rev. A **100**, 013614 (2019).

[20] Y. Sekino and Y. Nishida, Field-theoretical aspects of one-dimensional Bose and Fermi gases with contact interactions, Phys. Rev. A **103**, 043307 (2021).

[21] S. Tan, Three-boson problem at low energy and implications for dilute Bose-Einstein condensates, Phys. Rev. A **78**, 013636 (2008).

[22] S. Zhu and S. Tan, Three-body scattering hypervolumes of particles with short-range interactions, arXiv:1710.04147.

[23] P. M. A. Mestrom, V. E. Colussi, T. Secker, and S. J. J. M. F. Kokkelmans, Scattering hypervolume for ultracold bosons from weak to strong interactions, Phys. Rev. A **100**, 050702(R) (2019).

[24] P. M. A. Mestrom, V. E. Colussi, T. Secker, G. P. Groeneveld, and S. J. J. M. F. Kokkelmans, van der Waals Universality near a Quantum Tricritical Point, Phys. Rev. Lett. **124**, 143401 (2020).

[25] Z. Wang and S. Tan, Three-body scattering hypervolume of particles with unequal masses, Phys. Rev. A **103**, 063315 (2021).

[26] P. M. A. Mestrom, V. E. Colussi, T. Secker, J.-L. Li, and S. J. J. M. F. Kokkelmans, Three-body universality in ultracold p-wave resonant mixtures, Phys. Rev. A **103**, L051303 (2021).

[27] P. M. A. Mestrom, J.-L. Li, V. E. Colussi, T. Secker, and S. J. J. M. F. Kokkelmans, Three-body spin mixing in spin-1 Bose-Einstein condensates, Phys. Rev. A **104**, 023321 (2021).

[28] Z. Wang and S. Tan, Scattering hypervolume of spin-polarized fermions, Phys. Rev. A **104**, 043319 (2021).

[29] Z. Wang and S. Tan, Scattering hypervolume of fermions in two dimensions, Phys. Rev. A **106**, 023310 (2022).

[30] H.-W. Hammer and D. Lee, Causality and universality in low-energy quantum scattering, Phys. Lett. B **681**, 500 (2009).

[31] H.-W. Hammer and D. Lee, Causality and the effective range expansion, Ann. Phys. (NY) **325**, 2212 (2010).

[32] M. Girardeau, Relationship between systems of impenetrable bosons and fermions in one dimension, J. Math. Phys. **1**, 516 (1960).

[33] T. Cheon and T. Shigehara, Fermion-Boson Duality of One-Dimensional Quantum Particles with Generalized Contact Interactions, Phys. Rev. Lett. **82**, 2536 (1999).

[34] E. H. Lieb and W. Liniger, Exact analysis of an interacting Bose gas. I. The general solution and the ground state, Phys. Rev. **130**, 1605 (1963).

[35] H. Bethe, Zur theorie der metalle, Eur. Phys. J. A **71**, 205 (1931).

[36] J. B. McGuire, Study of exactly soluble one-dimensional n-body problems, J. Math. Phys. **5**, 622 (1964).

[37] L. Pricoupenko, Resonant Scattering of Ultracold Atoms in Low Dimensions, Phys. Rev. Lett. **100**, 170404 (2008).

[38] T. Kristensen and L. Pricoupenko, One-dimensional ultracold atomic gases: Impact of the effective range on integrability, Phys. Rev. A **93**, 023629 (2016).

[39] E. Braaten and H.-W. Hammer, Universality in few-body systems with large scattering length, Phys. Rep. **428**, 259 (2006).